Intersulfur Distance Is a Key Factor in Tuning Disulfide Radical Anion Vertical UV−Visible Absorption

ARTICLE *in* JOURNAL OF PHYSICAL CHEMISTRY LETTERS · JANUARY 2010

Impact Factor: 7.46 · DOI: 10.1021/jz900214e

3 AUTHORS:

Elise Dumont
Ecole normale supérieure de Lyon
52 PUBLICATIONS **612** CITATIONS
SEE PROFILE

Adèle D Laurent
University of Nantes
52 PUBLICATIONS **621** CITATIONS
SEE PROFILE

Xavier Assfeld
University of Lorraine
107 PUBLICATIONS **1,672** CITATIONS
SEE PROFILE

THE JOURNAL OF PHYSICAL CHEMISTRY Letters

pubs.acs.org/JPCL

Intersulfur Distance Is a Key Factor in Tuning Disulfide Radical Anion Vertical UV−Visible Absorption

Elise Dumont,*[,†] Adèle D. Laurent,[†] and Xavier Assfeld[†]

[†]Laboratoire de Chimie, UMR 5182, École Normale Supérieure de Lyon, 69364 Lyon Cedex 07, France and [†]Équipe Chimie et Biochimie Théoriques, UMR 7565 CNRS-UHP, Institut Jean Barriol, (FR CNRS 2843), Faculté des Sciences et Techniques, Nancy-Université, B.P. 70239, 54506 Vandoeuvre-lès-Nancy, France

ABSTRACT Maximum absorption wavelengths λ_{max} for $\sigma^* \leftarrow \sigma$ vertical transition of peptidic disulfide radical anions of increasing complexity were investigated by means of time-dependent density functional theory. Values among a representative set of 17 two-cysteinyl peptides range between 385 and 624 nm (TD-BH&HLYP/DZP++//MP2/DZP++:HF/6-31G* level of theory). This considerable spread contrasts with the usually admitted value of ca. 400−450 nm typically ascribed to two-center three-electron bonds. It is traced back to the large range of equilibrium intersulfur distances d, with values comprised between 2.73 and 3.19 Å. More quantitatively, blue- and red-shifts follow a near-linear regime (slope of 46 nm per 0.1 Å). They can be mapped onto a relaxed scan of L,L-cystine taken as a prototypical system λ_{max}^{ref} = 436 nm, 2.79 Å. This result could assist future radioprotectants rational design, with disulfide-linking arcs of controlled geometry. Meanwhile, the presence of a secondary structure motif such as an α-helix does not affect the UV−vis transition.

SECTION Molecular Structure, Quantum Chemistry, General Theory

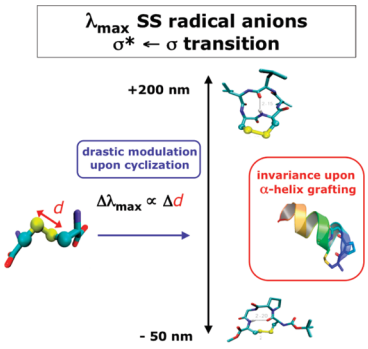

Disulfide radical anions (RAs) are ubiquitous in chemistry and biochemistry.[1] Numerous experimental evidence have ascertained their key role as metastable intermediates (disulfide:dithiol redox couple,[2] relay stations for electron transfer[3]). Their formation and outcome are proved to be both highly dependent on the environment and usually strongly asymmetric in biomolecules.[4−7] Neutral disulfide versatility has given rise to state-of-the-art applications such as folding of an α-helix[8] or two-dimensional infrared (2D-IR) monitoring of an hydrogen bond breaking.[9] *Cyclic* RA entities also possess an intrinsic malleability,[10] together with enhanced reactional and spectroscopic properties that could be tuned by designing precise molecular architectures.[11] They have been recently characterized in transition metal complexes[12−14] as interesting electron acceptor, with a real potential for triggering intramolecular electron transfer, excitation energy transfer, and the formation of long-lived charge-separated states in light-harvesting structures.[15] Another possible application of disulfide RA spectroscopy is the search for efficient radioprotectant (scavengers) conceived to protect biomolecules from specific damage, with attempts involving small organic compounds such as α-lipoic acid derivatives.[16] Designing such systems requires an in-depth knowledge of the exotic molecular nature of these intermediates, progressively built up since the pioneer work by Pauling.[17] Disulfide RAs are formed by nondissociative capture by a neutral disulfide bridge.[18] The excess electron is attached onto the low-lying antibonding σ^* orbital, forming a three-electron two-center (2c-3e) bond with a concomitant bond lenghtening of ca. 0.7 Å. Indeed, topological analysis confirm the formal bond order of one-half.[19] Elucidation of mechanistic pathways in which disulfide RAs are involved constitutes a whole line of research, deeply rooted in the existence of (more or less direct) experimental probes. Many techniques have been proposed for the proper identification of these elusive intermediates: electrochemistry,[20−22] X-ray crystallography,[6] electron paramagnetic resonance,[21,23] and Raman spectroscopy.[12] Yet, such techniques can be demanding and may not be applicable to a particular system. Stopped-flow UV−visible (UV−vis) monitoring has been used for more than three decades ago, and remains the most common procedure. A peak around 400 nm is usually ascribed to hemibonded molecular cations or anions (dihalogen,[24] disulfides,[1] or more generally S∴Y bonds[25] where Y = O, N, Se, ...). This transition has a strong $\sigma^* \leftarrow \sigma$ character, with an energy gap strongly decreased upon elongation. A continuous and marked red-shift from ca. 200 nm (also corresponding to the value of the neutral entity[26]) to 400 nm is induced (see Figure 1). Meanwhile, the signal intensity is considerably reinforced. The real-time probing of dimethyldisulfide (DMeDS) has been reported resorting to subpicosecond laser spectroscopy.[27] Fortunately enough, biological systems present larger lifetimes.[16] Quantum mechanics (QM)

Received Date: November 2, 2009
Accepted Date: December 26, 2009
Published on Web Date: January 07, 2010

DOI: 10.1021/jz900214e | *J. Phys. Chem. Lett.* **2010**, *1*, 581–586

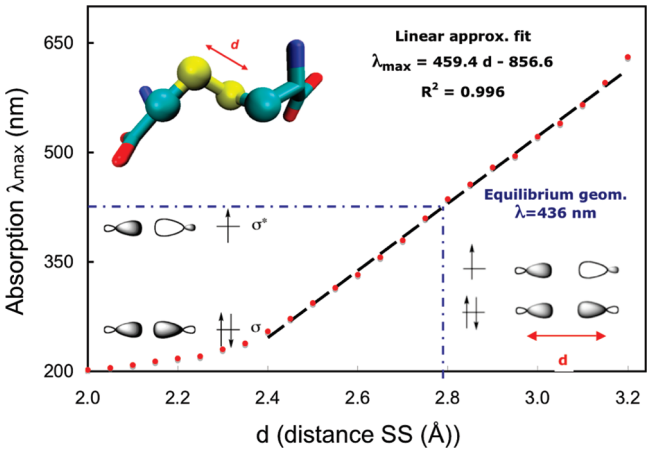

Figure 1. Maximum absorption wavelength λ_{max} for radical anionic L,L-cystine, as a function of the intersulfur distance d. Values follow a near-linear regime in the range 2.4−3.2 Å.

calculations often complement experimental detection of transient disulfide RAs, in order to confirm UV−vis assignment. The latter can be more delicate than it seems, as *"the absorption spectra of cyclic disulfide radical anions are subject to large variations in both the position of the maximum absorption wavelengths and the value of the molecular extinction coefficients"*.[28] In a recent theoretical study on analogue peptides presenting S∴Y radical cations, Bergès et al.[25] noticed a *"strong conformational dependence"* of λ_{max}. It is quite desirable to build up a sound understanding of the factors inducing a spectral tuning; in this letter, λ_{max} values are evaluated on a large set of molecules: dialkyldisulfides, L,L-cystine, and short-loop peptides. A neat geometrical dependence with the intersulfur distance, denoted d, is evidenced.

Maximum absorption wavelengths λ_{max} are computed for six symmetric dialkyldisulfides RSSR, named DRDS, with R = H, Me, Et, Pr, iPr, tBu (first subblock of Table 1). Variation along the first four systems (red shifts of +27, +10, +2 nm between two consecutive systems) follows the increasing inductive strength, as explained by Asmus et al., who reported a neat correlation between experimental absorption maxima and σ_I Taft's parameters.[29] Similarly, a +10 nm red-shift passing from diethyldisulfide (DEtDS) to DiPrDS is found. Yet, a stronger red-shift is predicted for ditertiobutyldisulfide (third hydrogen-to-methyl substitution, +24 nm). It indicates that electronic contributions do not solely impact λ_{max}, and DtBuDS presents a lengthening of 0.05 Å of the 2S−3e distance d, compared to other aliphatic compounds. A correlation between d and λ_{max} is a plausible hypothesis; it is further tested on L,L-cystine, a linear dipeptide that constitutes our reference system[30] hereafter (λ_{max}^{ref} = 436 nm, see Figure 1). The +15 nm red-shift compared to DEtDS arises from stereoelectronic effects of −CO and −NH groups. UV−vis absorption maxima of aliphatic linear systems and L,L-cystine lie in the usually admitted range of 400—450 nm. Its absorption λ_{max}^{ref} is now monitored as a function of d (relaxed scan) to evidence a geometrically induced spectral tuning.

A large range of intersulfur distances is explored (2.0—3.2 Å), along which λ_{max} drastically increases from 200 to 645 nm as shown on Figure 1; meanwhile, oscillator strengths are almost constant close to 0.30 after an initial increase (see SI). It is worth mentioning that Gauduel et al. managed to follow this continuous red-shift using subpicosecond photochemistry.[27] Variation of λ_{max} as a function of d is governed by the energy gap between the σ_{SS} and the σ^*_{SS} orbitals. This gap is related to the atomic orbital overlap (S). As S decreases exponentially with respect to the distance ($S \propto \exp(-d)$), one can write $\lambda_{max} = A\exp(B^*d) + C$. A regular fit provides

$$\lambda_{max} = 20.52\exp(1.072^*d) + 4.19 \quad (\text{in nm})$$
$$R^2 = 0.985 \quad d\in[2.0:3.2] \qquad (1)$$

On a slightly restricted d interval, $\exp(-d) \propto 1/d$ such that an approximate linear correlation can be proposed:

$$\lambda_{max} = 462.9d - 864.8 \quad (\text{in nm})$$
$$R^2 = 0.998 \quad d\in[2.4:3.2] \qquad (2)$$

While λ_{max} variation does not come as a surprise [The monotonous relation between absorption maxima and distance is not verified for small organic systems such as 1,2-dithia-cycloalkanes. The drastic ring strain indeed leads to a mixing of MOs, as discussed by Maity on disulfide radical cations[31]], the slope in eq 2 implies that considerable blue or red shifts can be achieved, since hemibonded systems are highly malleable.[10,32] For convenience, one can propose a rule of thumb to estimate them, with a deviation of 46 nm per 0.1 Å knowing that λ_{max}^{ref} = 436 nm for d = 2.79 Å. At this stage, we have evidenced a clear geometrical dependence on a constrained prototypical disulfide RA. As a corollary, it indirectly explains the $\lambda_{max} = f(\tau)$ torsional profile, with a dissymmetric U-shaped curve obtained for DMeDS (see SI). Weaker red shifts for *cis* or *trans* forms from the equilibrium angle (84.3°), account for +29 and +11 nm since the distance increases accordingly. We also recently reported a similar correlation for absorption of RA DMeDS:xH$_2$O clusters (microhydration, $x \leq 5$) arising from a mechanical embedding of the water subcluster.[33] In this letter, this simple rule is tested on biological systems, belonging to a representative set of 17 peptides of generic sequence Cys-(Xxx)$_n$-Cys, $n \leq 5$. The latter was built up in ref 10. They are listed in Table 1, together with characteristic geometric parameters and calculated λ_{max}.. Such short-loop motifs are widely studied in the literature, with a particular focus on understanding how the inner peptide (Xxx)$_n$ induces drastic modulations of disulfide bridge reactivity.[34,35] This remarkable variety allows one to build up a representative set within a limited number of peptides.[10] The intersulfur distance d of disulfide RAs is a highly malleable parameter, with values ranging between 2.73 and 3.19 Å for **3b** and **1**. A clear rationalization of the geometrical interplay between the 2S−3e linkage and its inner −(Xxx)$_n$− arc is delicate, but the following tendencies can be pointed out: (i) For the biologically most frequent case (n = 2), the alanine-to-proline inner mutation (compounds **3a**, **3b**, and **3c**) tends to shorten d by 0.05—0.07 Å, because of a different β-turn type [Proline presence is crucial in oxidoreductases, as it distinguishes thioredoxins from glutaredoxines]. (ii) Conversely, disulfide RAs embedded within Cys-Cys loops (n = 0) are

DOI: 10.1021/jz900214e | J. Phys. Chem. Lett. 2010, 1, 581–586

Table 1. Geometries and Absorptions λ_{max} of 17 Short-Loop Peptides Featuring a Three-Electron Two-Center Disulfide Linkage

			structure			spectroscopy		
compound	m^a	n^a	d(S−S)	∠(CSS)	τ(CSSC)	λ_{max} in nm (f)	$\Delta\lambda_{max}{}^b$	% ($\sigma^* \leftarrow \sigma$)^c
				Aliphatic Linear Compounds				
S_2H_2			2.81	85.9	102.2	383 (0.53)		0.774
DMeDS			2.79	87.4	84.3	411 (0.36)		0.832
DEtDS			2.79	88.6	85.3	421 (0.38)		0.824
DPrDS			2.79	88.7	107.6	423 (0.36)		0.873
DiPrDS			2.80	90.2	129.0	432 (0.40)		0.854
DtBuDS			2.85	95.5	122.0	456 (0.37)		0.824
L,L-Cys			2.79	95.4	82.3	436 (0.31)		0.881
				Cys-Cys Motifs				
NHMe-Cys-Cys-Boc (**0a**)	2	0	2.94	90.6, 95.5	102.8	493 (0.28)	0.7	0.845
Malformin (**1**)^d	5	0	3.19	95.9, 100.0	91.4	624 (0.24)	14.6	0.825
Helix (**2**) Cys-Gly_{14}-Cys	16	0	2.89	97.4, 106.4	47.3	483 (0.27)	10.1	0.809
				Cys-Xxx-Cys motif				
Cys-Ala-Cys (**0b**)	3	1	2.84	86.2, 105.1	163.8	411 (0.25)	−7.5	0.789
				Cys-Xxx_2-Cys Motif				
Cys-Ala-Ala-Cys (**0c**)	4	2	2.80	88.6, 88.7	83.1	439 (0.38)	9.6	0.794
Cys-Pro-Aib-Cys (**3a**)	4	2	2.75	94.4, 99.0	106.5	412 (0.35)	5.3	0.804
Cys-Pro-Phe-Cys (**3b**)	4	2	2.73	89.0, 95.0	118.2	385 (0.34)	−12.2	0.827
Cys-Pro-Gly-Cys (**3c**)	4	2	2.73	93.9, 88.3	122.5	386 (0.34)	−11.8	0.843
Pen-Pro-Aib-Cys (**3d**)	4	2	2.77	101.4, 110.7	112.6	435 (0.35)	19.2	0.823
Cys-Pro-Aib-Pen (**3e**)	4	2	2.81	96.3, 111.8	102.4	443 (0.33)	8.4	0.848
Pen-Pro-Aib-Pen (**3f**)	4	2	2.87	114.1, 111.4	107.5	510 (0.33)	48.1	0.874
Cys-Phe-Gly-Cys-Gly (**3g**)	5	2	2.85	88.3, 96.4	66.9	438 (0.34)	−14.6	0.818
				Cys-Xxx_3-Cys Motif				
Cys-Ala_3-Cys (**0d**)	5	3	2.83	91.1, 94.4	135.4	441 (0.30)	2.3	0.915
				Cys-Xxx_4-Cys Motif				
Cys-Ala_4-Cys (**0e**)	6	4	2.85	88.4, 89.9	85.2	456 (0.37)	3.4	0.808
Hairpin (**4**)^e	6	4	2.73	115.6, 97.3	78.9	394 (0.26)	−3.5	0.853
Oxytocin (**5**)^f	9	4	2.80	103.2, 119.1	61.1	440 (0.34)	10.3	0.861
				Cys-Xxx_5-Cys Motif				
Cys-Ala_5-Cys (**0f**)	7	5	2.80	87.5, 108.6	97.7	437 (0.28)	6.9	0.874

[a] m corresponds to the total number of residues for a given peptide, and n is the number of residues forming the Cys-Cys loop. [b] λ_{max} values are computed by the difference between the calculated λ_{max} and the value extrapolated from the linear L,L-cystine baseline. [c] Weight of the $\sigma^* \leftarrow \sigma$ doublet state. [d] Sequence cyclo-D-Cys-D-Cys-L-Val-D-Leu-L-Ile [e] Boc-Cys-Val-Aib-Ala-Leu-Cys-NHMe; taken from ref 40. [f] Cys-Tyr-Phe-Glu-Asp-Cys-Pro-Arg-Gly.

systematically lenghtened by at least 0.1 Å compared to the reference L,L-cystine. Malformin (**1**) is the most striking example (d = 3.19 Å). An elongation of the 2S−3e bond is also induced by the double Cys → Pen mutation (**3f**) (Pen denotes the nonstandard amino acid penicillamine (β,β-dimethyl cysteine)); the latter elongation is analogous to the one found for DtBuDS (direct and local replacement of $-CH_2-S$ groups by $-C(CH_3)_2-S$).

This mechanical embedding turns out to be decisive for maximum absorption wavelengths λ_{max}, which span a very large range of values (between 385 and 624 nm). Extrema respectively correspond to **3b** and **1**, that is, precisely peptides presenting the most drastic modulation of the intersulfur distance d (2.75 and 3.19 Å). λ_{max} of these 17 peptides verify eq 2 with a mean unsigned error of 11.1 nm (averaged relative error of 4.9 nm), which is acceptable considering the large range described. Peptides showing the most critical deviations ($\Delta\lambda_{max}$), defined as the difference between the calculated λ_{max} and the value extrapolated from the linear L,L-cystine baseline, are labeled on Figure 2.

One notes that Pen-containing peptides (**3d**, **3e**, **3f**), are systematically red-shifted by at least 8 nm compared to the L,L-cystine baseline, denoting additional inductive effects from methyl groups that bias a mapping with the Cys-containing reference. Conversely, phenylalanine (Phe, the sole aromatic residue of our set) occurrence within the linking arc **3b** and **3g** results in a −10 nm offset with respect to the baseline. Inspection of molecular orbitals implied in the transition

DOI: 10.1021/jz900214e | J. Phys. Chem. Lett. 2010, 1, 581–586

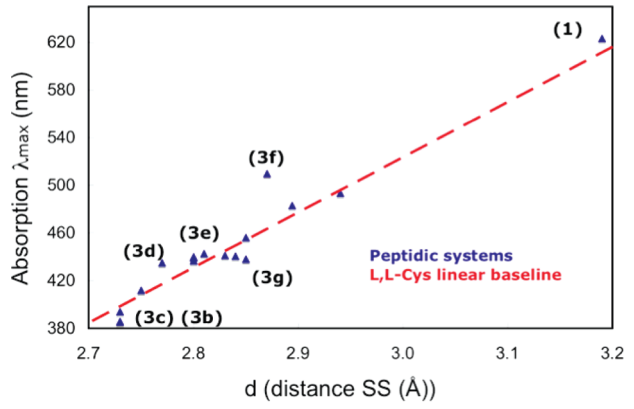

Figure 2. Maximum absorption wavelengths λ_{max} for a series of short-loop disulfide-linked peptides (blue triangles), as a function of d. The near-linear fit (eq 2, red dashed line) is added as a baseline. Peptides presenting largest deviations $\Delta\lambda_{max}$ are labeled and discussed in the main text.

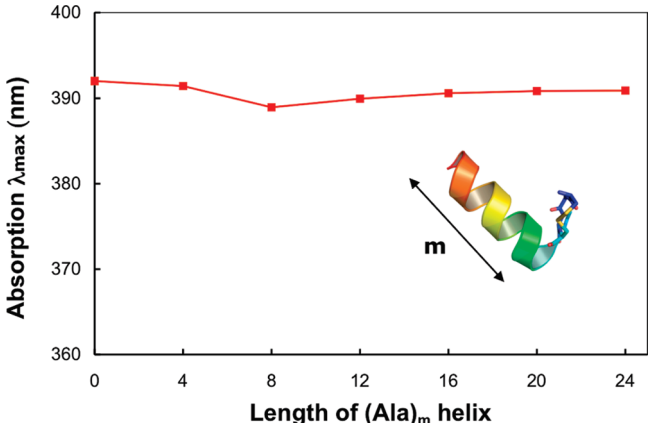

Figure 3. Stability of maximum absorption wavelengths λ_{max} along the peptidic series Ala_m-Cys-Pro-Gly-Cys peptide ($m \leq 24$, with a four-periodicity).

indicates a small mixing with the $\pi^* \leftarrow \pi$ phenylic transition (smaller oscillator strength $f = 0.12$). As a simple test, it can be verified that agreement is restored for a phenylalanine-to-alanine mutation at frozen geometries, ($\Delta\lambda_{max}$ (**3b**) passes from −12 to −3 nm, and $\Delta\lambda_{max}$ (**3g**) from −15 to −6 nm).

Not only inner but also outer residues can potentially induce a spectral tuning, notably by defining secondary or tertiary structures. Its crucial effect on $\pi^* \leftarrow \pi$ dyes embedded in complex biomolecules has been traced back to dipole−dipole interactions.[36,37] As a simple test, an alanine homopolymer (m residues) in an α-helix conformation (thus $m \geq 4$) is grafted onto the Cys-Pro-Gly-Cys tetrapeptide (**3c**). Its structure is depicted in Figure 3, and λ_{max} is monitored as a function of m, with a four-periodicity. Corresponding numerical data and geometrical parameters of the 2S−3e linkage are reported in the Supporting Information (Table II). The latter remain highly stable with respect to the isolated tetrapeptide ($m = 0$). A systematic but slight blue-shift (less than −3 nm) is induced: it reflects similar charge−dipole interactions for ground and first excited states. Thus λ_{max} exhibits a very limited sensitivity toward α-helix presence.

In this work, it is demonstrated how *cyclic* peptidic disulfide RAs optical properties intimately depend on the geometry of the linking arc $-(Xxx)_n-$, which is a direct consequence of the remarkable malleability of such hemibonds. In spite of the diversity of mutations explored, a simple geometrical dependence with the intersulfur distance is evidenced: a parallel can be drawn with the torsional dependence for $\pi^* \leftarrow \pi$ transitions. Maximum absorption wavelengths λ_{max} values can be extrapolated from a simple scan of the prototypical L,L-cystine with a good precision. Largest deviations can be traced to additional electronic contributions (adjacent methyl or aromatic substituents), inducing either blue or red shifts. Conversely, collective electrostatic effects, such as an α-helix's dipole barely affects the UV−vis signature of disulfide RAs. Generalization of these rules to other three-electron two-center systems, notably dissymmetric ones such as S∴Y, will be examined in the near future.

METHODS

Geometries of aliphatic disulfides and L,L-cystine were optimized at the MP2/DZP++ level of theory. Geometries of peptidic RAs were optimized at the ONIOM[38] (MP2/DZP++:HF/6-31G*) level of theory, starting with initial structures taken from ref 10; cartoon representations are also given. The high-level description of the limited $-CH_2-S-S-CH_2-$ moiety; this proximal boundary was duly calibrated and only introduces a constant energetic offset. Vertical absorption energies were computed within the framework of time-dependent density functional theory (TD-DFT). The hybrid half-and-half BH&HLYP functional[39] was used, as it provides a reliable description of three-electron two-center bond vertical absorptions.[25,31] Full TD-DFT calculations are no longer amenable when considering an α-helix, but its electrostatic effects can be accurately described by molecular mechanics (MM). Special care was taken to ensure a near-optimal QM/MM description; full details are given in the Supporting Information. Solvent effects were not systematically introduced in this study, since test calculations on DMeDS and L,L-cystine (Supporting Information) establish a constant shift of +20 nm. The underlying assumption is that solvent effects are adequately compensated by the use of bound-state basis functions, resulting in the cancellation of errors.

SUPPORTING INFORMATION AVAILABLE Additional details on the QM/MM schemes for optimization and optical properties calculations. Table of geometrical parameters and λ_{max} values for Figures 1 and 3. Torsional dependence of λ_{max} for dimethylsulfide RA (gas-phase and phase change material (PCM)). This material is available free of charges via the Internet at http://pubs.acs.org.

AUTHOR INFORMATION

Corresponding Author:

*To whom correspondence should be addressed. E-mail: elise.dumont@ens-lyon.fr.

ACKNOWLEDGMENT Ab initio calculations were performed using the local HPC resources of PSMN at ENS-Lyon and of GENCI (CINES/IDRIS), Project x2009075105. Nicolas Ferré (Univ. Provence) is

DOI: 10.1021/jz900214e | J. Phys. Chem. Lett. 2010, 1, 581–586

kindly acknowledged for a local version of the link atom scheme. The authors sincerely thank Dr. Pierre-François Loos for seminal discussions and comments on the manuscript. A.D.L. and X.A. acknowledge financial support from the Jean Barriol Institute (FR CNRS 2843).

REFERENCES

(1) Asmus, K. D. Stabilization of Oxidized Sulfur Centers in Organic Sulfides. Radical Cations and Odd Electron Sulfur-Sulfur Bonds. *Acc. Chem. Res.* **1979,** *12*, 436–442.

(2) Kemp, M.; Go, Y.-M.; Jones, D. P. Nonequilibrium Thermodynamics of Thiol/Disulfide Redox Systems: A Perspective on Redox Systems Biology. *Free Radic. Biol. Med.* **2008,** *44*, 921–937.

(3) Chen, X.; Zhang, L.; Wang, Z.; Li, J.; Wang, W; Bu., Y. Relay Stations for Electron Hole Migration in Peptides: Possibility for Formation of Three-Electron Bonds along Peptide Chains. *J. Phys. Chem. B* **2008,** *112*, 14302–14311.

(4) Bergès, J.; Rickards, G.; Rauk, A.; Houée-Levin, C. QM/MM Study of Electron Addition on Protein Disulfide Bonds. *Chem. Phys. Lett.* **2006,** *421*, 63–67.

(5) Sawicka, A.; Skurski, P.; Simons, J. Excess Electron Attachment to Disulfide-Bridged L,L-Cystine. An Ab Initio Study. *J. Phys. Chem. A* **2004,** *108*, 4261–4268.

(6) Weik, M.; Ravelli, R. B.; Silman, I.; Sussman, J. L.; Gros, P.; Kroon, J. Synchrotron X-ray Radiation Produces Specific Chemical and Structural Damage to Protein Structures. *Proc. Natl. Acad. Sci. U.S.A.* **2000,** *97*, 623–628.

(7) Rickard, G. A.; Bergès, J.; Houée-Levin, C.; Rauk, A. Ab Initio and QM/MM Study of Electron Addition on the Disulfide Bond in Thioredoxin. *J. Phys. Chem. B* **2008,** *112*, 5774–5787.

(8) Lu, H. S. M.; Volk, M.; Kholodenko, Y.; Gooding, E.; Hochstrasser, R. M.; Degrado, W. F. *J. Am. Chem. Soc.* **1997,** *119*, 7173–7180.

(9) Kolano, C.; Helbing, J.; Kozinski, M.; Sander, W.; Hamm, P. Watching Hydrogen Bond Dynamics in a β-Turn by Transient 2D-IR Spectroscopy. *Nature* **2006,** *444*, 469–472.

(10) Dumont, E.; Loos, P.-F.; Assfeld, X. Factors Governing Electron Capture by Small Disulfide Loops in Two-Cysteine Peptides. *J. Phys. Chem. B* **2008,** *112*, 13661–13669.

(11) Wenska, G.; Filipiak, P.; Asmus, K. D.; Bobrowski, K.; Koput, J.; Marciniak, B. *J. Phys. Chem. B* **2008,** *112*, 10045–10053.

(12) Melnikov, M. Ya.; Weinstein, J. A. Structural Reorganization in the Excited State of Transition Metal Complexes. *High Energy Chemistry* **2008,** *42*, 329–331.

(13) Ragsdale, S. W. Nickel-Based Enzyme Systems. *J. Biol. Chem.* **2009,** *284*, 18571–18575.

(14) Pal, P. K.; Drew, M. G. B.; Datta, D. Tuning of Intramolecular Electron Transfer between Ru(II) and the Disulfide Bond. *New J. Chem.* **2003,** *27*, 197–201.

(15) Albinsson, B.; Martensson, J. Long-Range Electron and Excitation Energy Transfer in Donor−Bridge−Acceptor Systems. *J. Photochem. Photobiol. C* **2008,** *9*, 138–155.

(16) McGeehan, J.; Ravelli, R. B. G.; Murray, J. W.; Owen, R. L.; Cipriani, F.; McSweeney, S.; Weik, M.; Garman, E. F. Colouring Cryo-Cooled Crystals: On-Line Microspectrophotometry. *J. Synchrotron Radiat.* **2009,** *16*, 163–172.

(17) Pauling, L. The Nature of the Chemical Bond. *J. Am. Chem. Soc.* **1931,** *53*, 1367–1400.

(18) Carlés, S.; Lecomte, F.; Schermann, J.-P.; Desfrancois, C.; Xu, S.; Milles, J. M.; Bowen, K. H.; Bergès, J.; Houée-Levin, C. *J. Phys. Chem. A* **2001,** *105*, 5622–5626.

(19) Fourré, I.; Silvi, B. What Can We Learn from Two-Center Three-Electron Bonding with the Topological Analysis of ELF? *Het. Chem.* 2007, *18*, 135−160.

(20) Antonello, S.; Benassi, R.; Gavioli, G.; Taddei, F.; Maran, F. Theoretical and Electrochemical Investigation on Dissociative Electron Transfers Proceeding Through the Formation of Loose Radical Anion Species: Reduction of Symmetrical and Unsymmetrical Disulfides. *J. Am. Chem. Soc.* **2002,** *124*, 7529–7538.

(21) Johnson, D. L.; Polyak, S. W.; Wallace, J. C.; Martin, L. L. Probing the Stability of the Disulfide Radical Intermediate of Thioredoxin Using Direct Electrochemistry. *Pept. Sci.* **2003,** *10*, 495–500.

(22) Chai, C. L. L.; Heath, G. A.; Huleatt, P. B.; O'Shea, G. A. The First Electrochemical Study of Epidithiopiperazine-2,5-diones, a Special Class of α,α-Disulfide Bridged Cyclic Dipeptides. *J. Chem. Soc., Perkin Trans. 2* **1999,** 389–391.

(23) Lawrence, C. C.; Bennati, M.; Obias, H. V.; Bar, G.; Griffin, R. G.; Stubbe, J. High-Field EPR Detection of a Disulfide Radical Anion in the Reduction of Cytidine 5′-Diphosphate by the E441Q R1 Mutant of *Escherichia coli* Ribonucleotide Reductase. *Proc. Natl. Acad. Sci. U.S.A.* **1999,** *96*, 8979–8984.

(24) Tung, T.-L.; Stone, J. A. The Formation and Reactions of Disulfide Radical Anions in Aqueous Solution. *Can. J . Chem.* **1975,** *53*, 3153–3157.

(25) Fourré, I.; Bergès, J.; Braida, B.; Houée-Levin, C. Topological and Spectroscopic Study of Three-Electron Bonded Compounds As Models of Radical Cations of Methionine-Containing Dipeptides. *Chem. Phys. Lett.* **2008,** *467*, 164–169.

(26) Rauk, A. Chiroptical Properties of Disulfides. Ab Initio Studies of Dihydrogen Disulfide and Dimethyl Disulfide. *J. Am. Chem. Soc.* **1984,** *106*, 6517–6524.

(27) Gauduel, Y.; Launay, T.; Hallou, A. Femtosecond Probing of a 2c/3e Disulfide Bond Making in Liquid Phase. *J. Phys. Chem. A* **2002,** *106*, 1727–1732.

(28) Southworth-Davies, R. J.; Garman, E. F. Radioprotectant Screening for Cryocrystallography. *J. Synchrotron Radiat.* **2007,** *14*, 73–83.

(29) Goebl, M.; Bonifacic, M.; Asmus, K. D. *J. Am. Chem. Soc.* **1984,** *106*, 5988–5992.

(30) Dumont, E.; Laurent, A. D.; Loos, P.-F.; Assfeld, X. Analysing the Selectivity and Successiveness of a Two-Electron Capture on a Multiply Disulfide-Linked Protein. *J. Chem. Theor. Comput.* **2009,** *5*, 1700–1709.

(31) Maity, D. K. Structure, Bonding, and Spectra of Cyclic Dithia Radical Cations: A Theoretical Study. *J. Am. Chem. Soc.* **2002,** *124*, 8321–8328.

(32) Geronimo, I. M.; Chéron, N.; Fleurat-Lessard, P.; Dumont, E. How Does Microhydration Impact on Structure, Spectroscopy and Formation of Disulfide Radical Anions? An Ab Initio Investigation on Dimethyldisulfide. *Chem. Phys. Lett.* **2009,** *481*, 173–179.

(33) Dumont, E.; Loos, P.-F.; Assfeld, X. Effect of Ring Strain on Disulfide Electron Attachment. *Chem. Phys. Lett.* **2008,** *458*, 276–280.

(34) Chivers, P. T.; Prehoda, K. E.; Raines, R. T. The CXXC Motif: A Rheostat in the Active Site. *Biochemistry* **1997,** *36*, 4061–4066.

(35) Carvalho, A. T. P.; Fernandes, P. A.; Swart, M.; Van Stralen, J. N. P.; Bickelhaupt, F. M.; Ramos, M. J. Role of the Variable Active Site Residues in the Function of Thioredoxin Family Oxidoreductases. *J. Comput. Chem.* **2008,** *30*, 710–724.

(36) Loos, P.-F.; Préat, J.; Laurent, A. D.; Michaux, C.; Jacquemin, D.; Perpète, E. A.; Assfeld, X. Theoretical Investigation of the

Geometries and UV/Vis Spectra of Poly(L-glutamic acid) Featuring Photochromic Azobenzene Side Chain. *J. Chem. Theor. Comput.* **2008,** *4*, 635–645.

(37) Strambi, A.; Coto, P. B.; Frutos, L. M.; Ferré, N.; Olivucci, M. Relationship between the Excited State Relaxation Paths of Rhodopsin and Isorhodopsin. *J. Am. Chem. Soc.* **2008,** *130*, 3382–3388.

(38) Vreven, T.; Morokuma, K. On the Application of the IMOMO (Integrated Molecular Orbital + Molecular Orbital) Method. *J. Comput. Chem.* **2000,** *21*, 1419–1432.

(39) Becke, A. D. A New Mixing of Hartree−Fock and Local Density-Functional Theories. *J. Chem. Phys.* **1993,** *98*, 1372–1377.

(40) Karle, I. L.; Kishore, R.; Raghothama, S.; Balaram, B. Cyclic Cystine Peptides. Antiparallel β-Sheet Conformation for the 20-Membered Ring in Boc-Cys-Val-Aib-Ala-Leu-Cys-NHMe. *J. Am. Chem. Soc.* **1988,** *110*, 1958–1963.

DOI: 10.1021/jz900214e | *J. Phys. Chem. Lett.* **2010,** *1*, 581–586